5032 J. Med. Chem. 2009, 52, 5032–5043
DOI: 10.1021/jm900528d

Journal of Medicinal Chemistry Article

Impact of Metal Coordination on Cytotoxicity of 3-Aminopyridine-2-carboxaldehyde Thiosemicarbazone (Triapine) and Novel Insights into Terminal Dimethylation

Christian R. Kowol,[†] Robert Trondl,[†] Petra Heffeter,[‡] Vladimir B. Arion,*[,†] Michael A. Jakupec,[†] Alexander Roller,[†] Markus Galanski,[†] Walter Berger,[‡] and Bernhard K. Keppler*[,†]

[†]*University of Vienna, Institute of Inorganic Chemistry, Währinger Strasse 42, A-1090 Vienna, Austria, and* [‡]*Department of Medicine I, Institute of Cancer Research, Medical University of Vienna, Borschkegasse 8a, A-1090 Vienna, Austria*

Received April 24, 2009

The first metal complexes of 3-aminopyridine-2-carboxaldehyde thiosemicarbazone (Triapine) were synthesized. Triapine was prepared by a novel three-step procedure in 64% overall yield. In addition, a series of related ligands, namely, 2-formylpyridine thiosemicarbazone, 2-acetylpyridine thiosemicarbazone, 2-pyridineformamide thiosemicarbazone, and their N^4-dimethylated derivatives (including the N^4-dimethylated analogue of Triapine) were prepared, along with their corresponding gallium(III) and iron(III) complexes with the general formula $[M(L)_2]^+$, where HL is the respective thiosemicarbazone. The compounds were characterized by elemental analysis, ^{1}H and ^{13}C NMR, IR and UV−vis spectroscopies, mass spectrometry, and cyclic voltammetry. In addition, Triapine and its iron(III) and gallium(III) complexes were studied by X-ray crystallography. All ligands and complexes were tested for their in vitro antiproliferative activity in two human cancer cell lines (41M and SK-BR-3), and structure−activity relationships were established. In general, the coordination to gallium(III) increased the cytotoxicity while the iron(III) complexes show reduced cytotoxic activity compared to the metal-free thiosemicarbazones. Selected compounds were investigated for the capacity of inhibiting ribonucleotide reductase by incorporation of ^{3}H-cytidine into DNA.

Introduction

Thiosemicarbazones are versatile ligands, as they adopt various binding modes with transition and main group metal ions.[1] They can act as mono- or bidentate ligands,[2] and their coordination capacity can be further increased, if aldehydes or ketones which contain additional functional group(s) in position(s) suitable for chelation are used for their preparation.[3,4] Besides their exciting coordination chemistry, thiosemicarbazones are known to possess a wide range of pharmaceutical properties such as antitumor, antiviral, antifungal, antibacterial, and antimalarial activity.[5] In addition, ^{64}Cu-bis(thiosemicarbazonate) complexes are under investigation as hypoxia-selective positron emission tomography tracers.[6] The first thiosemicarbazone with antitumor properties, namely, 2-formylpyridine thiosemicarbazone, was reported about 50 years ago.[7] Further studies showed that a prerequisite for biological activity is a nitrogen heterocycle that contains a suitable functional group for condensation with thiosemicarbazide derivatives at the α-position.[8] 5-Hydroxy-2-formylpyridine thiosemicarbazone (5-HP) was the first compound of this series that entered phase I clinical trials. However, 5-HP is rapidly transformed in the body and eliminated as an inactive glucuronide conjugate.[9,10] In addition, 5-HP showed severe hematological and gastrointestinal side effects that prevented its further clinical development. The currently most promising thiosemicarbazone as antitumor agent is 3-aminopyridine-2-carboxaldehyde thiosemicarbazone (Triapine[a]), which entered several phase I and phase II clinical trials.[11−15]

As the principal molecular target of α-N-heterocyclic thiosemicarbazones, the enzyme ribonucleotide reductase (RR) has been identified.[16−18] This enzyme catalyzes the conversion of ribonucleotides into deoxyribonucleotides, providing the precursors required for DNA synthesis and repair. α-N-Heterocyclic thiosemicarbazones are the most potent inhibitors of RR known so far. They are several orders of magnitude more effective than hydroxyurea, the first clinically applied RR inhibitor.[19] Faster proliferation of tumor cells compared to normal cells and therefore higher expression of RR make this enzyme a suitable and well established target in cancer chemotherapy.[20] The human RR consists of two homodimeric subunits: R1 and R2. The first subunit harbors the nucleotide binding site and the second subunit a diiron center and a tyrosyl radical. Transfer of the radical electron from tyrosine of R2 occurs by a proton-coupled mechanism via a chain of hydrogen-bonded amino acids over a distance of 35 Å to a cysteine of the R1 subunit, where it generates a thiyl radical essential for reduction of the substrates.[21] Recently, a second R2 subunit, called p53R2, has been identified in human cells with ∼80% sequence homology with R2 but with p53-dependent expression.[22] The p53 protein actively

*To whom correspondence should be addressed. For V.B.A.: phone, +431427752615; fax, +431427752680; e-mail, vladimir.arion@univie.ac.at. For B.K.K.: phone, +431427752600; fax, +431427752680; e-mail, bernhard.keppler@univie.ac.at.

[a] Abbreviations: Triapine, 3-amino-2-carboxaldehyde thiosemicarbazone; RR, ribonucleotide reductase; DFO, desferrioxamine; ROS, reactive oxygen species.

 Published on Web 07/28/2009

Scheme 1. Library of the Synthesized Compounds[a]

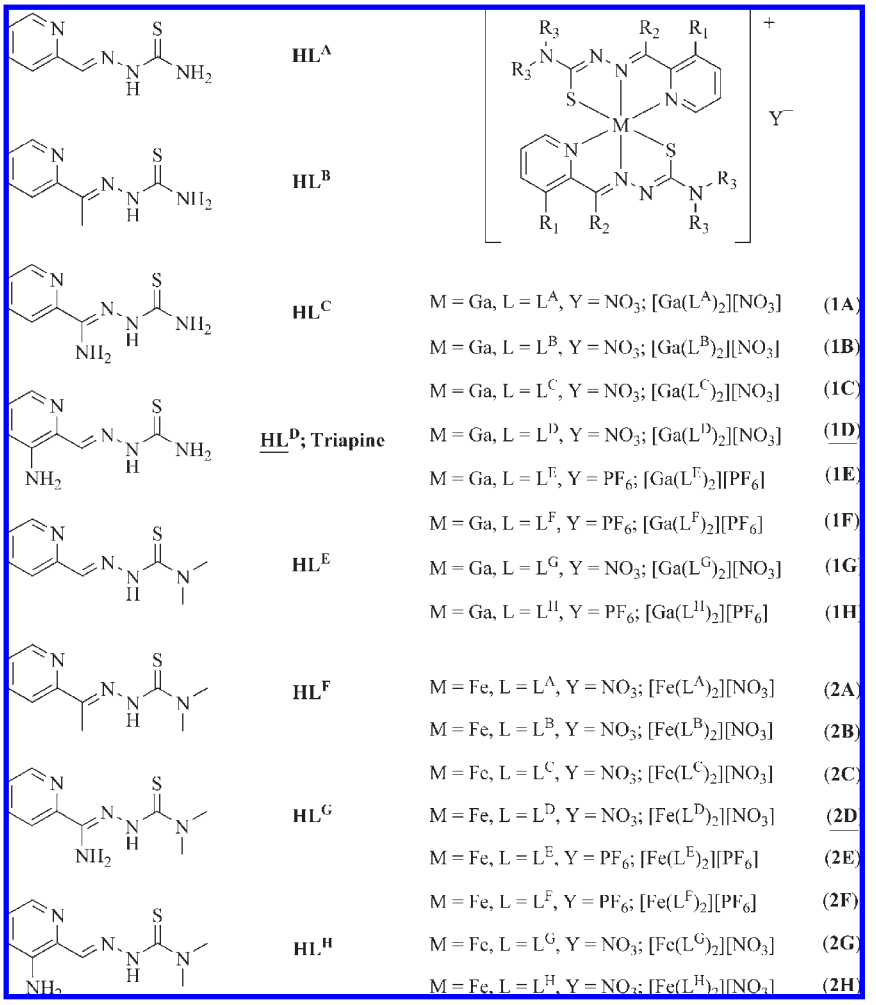

[a] Underlined species were studied by X-ray crystallography.

suppresses tumor formation, and the majority of human tumors have been found to contain mutations in p53 or defects in the pathways responsible for its activation.[23] Thus, the discovery of p53R2 revealed a link between the most important tumor suppressor and the synthesis of deoxyribonucleotides.

We reported previously that the gallium(III) complexes of N^4-disubstituted α-N-heterocyclic thiosemicarbazones (HL) with the composition $[Ga(L)_2]^+$ exhibit enhanced cytotoxicity in the low nanomolar range in human cancer cell lines. In contrast, the corresponding iron(III) complexes displayed a much lower cytotoxicity (in the micromolar range) than the metal-free ligands.[24] EPR measurements on isolated mouse R2 subunits of RR showed that the effects of the complexation to gallium(III) and iron(III) on the destruction of the R2 specific tyrosine free radical in the presence of the reductant dithiothreitol (DTT) are in the reverse order. The iron(III) complexes show the fastest destruction of the tyrosyl radical in RR, followed by the metal-free ligands and the corresponding gallium(III) complexes.[24] In the case of Triapine, iron also enhances radical quenching.[25] However, in contrast to N^4-dimethylated α-N-heterocyclic thiosemicarbazones, addition of iron(III) to Triapine results only in small changes in cytotoxicity.[26,27]

In order to evaluate the effect of complexation on the cytotoxicity of Triapine, the gallium(III) and iron(III) complexes were synthesized for the first time. For elucidation of further structure−activity relationships, a series of related ligands and their corresponding gallium(III) and iron(III) complexes were prepared (Scheme 1). In particular, the effects of the amino group and its position as well as the influence of N^4-disubstitution on cytotoxicity were investigated, including the Triapine analogue 3-aminopyridine-2-carboxaldehyde N^4-dimethylthiosemicarbazone. In addition, selected compounds were tested for their capacity of inhibiting ribonucleotide reductase by a ^{3}H-cytidine DNA incorporation assay.

Results and Discussion

Syntheses. The first reported synthesis of Triapine with an overall yield of 9% (six steps) started from 2-chloro-3-nitropyridine (Scheme S1; see Supporting Information).[28] An improved five-step synthesis[29] starting from the same material, via a Suzuki coupling in the first step, afforded 2-methyl-3-nitropyridine, which was further converted into an enamine intermediate. Oxidation of the latter led to 3-nitropyridine-2-carboxaldehyde, which was then reacted with thiosemicarbazide. In the final step the nitro derivative was reduced to Triapine in an overall yield of 55% (Scheme S2). The best overall yield of 64% was achieved in a four-step synthesis.[30] 3-Amino-2-chloropyridine was converted via a

Scheme 2. Novel Synthetic Pathway to Triapine ($\mathbf{HL^D}$)[a]

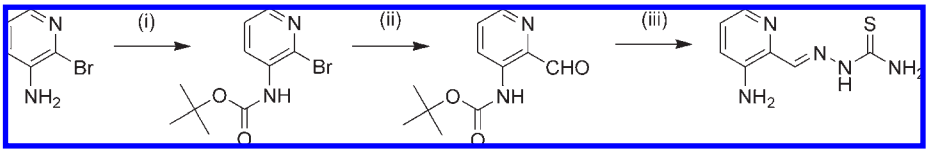

[a] Reagents and conditions: (i) sodium bis(trimethylsilyl)amide (~1 M/THF), $(Boc)_2O$, 82%; (ii) *n*-BuLi, *N*-formylpiperidine, 86%; (iii) thiosemicarbazide, conc HCl, $NaHCO_3$, 91%, overall yield 64%.

Heck reaction using styrene, followed by protection of the NH_2 group and then ozonolysis to the desired carboxaldehyde. The latter was transformed into Triapine by condensation with thiosemicarbazide and deprotection (Scheme S3). In this study, we developed a novel straightforward three-step synthesis of Triapine ($\mathbf{HL^D}$) in 64% overall yield, starting from the commercially available 3-amino-2-bromopyridine as shown in Scheme 2.

In the first step the amino group was protected with di-*tert*-butyl dicarbonate in dry THF, using sodium bis(trimethylsilyl)amide[31] as a base. Treatment of the *tert*-Boc protected 3-amino-2-bromopyridine with *n*-BuLi in dry THF resulted in the lithiated species, which was further reacted with *N*-formylpiperidine to give the carboxaldehyde.[32] Finally, the condensation reaction with thiosemicarbazide in ethanol in the presence of concentrated HCl afforded Triapine hydrochloride, which was converted into the free base ($\mathbf{HL^D}$) by treatment with sodium bicarbonate.[29] The Triapine analogue 3-aminopyridine-2-carboxaldehyde N^4-dimethylthiosemicarbazone ($\mathbf{HL^H}$) was prepared in 84% yield by using the same protocol. However, the conversion into the free base was performed by treatment of the hydrochloride with excess *N*-methylmorpholine.

The gallium(III) complexes $[Ga(L^A)_2]^+$ (**1A**) and $[Ga(L^D)_2]^+$ (**1D**) were prepared by reaction of $Ga(NO_3)_3 \cdot 9H_2O$ with the corresponding ligand ($\mathbf{HL^A}$ or $\mathbf{HL^D}$) in methanol in the presence of $NaOCH_3$ or triethylamine as a base in 27% and 72% yields, respectively (Scheme 1). The ^{1}H NMR spectra of these two complexes showed the presence of 0.5 and 0.15 equiv of methanol, correspondingly, in accord with the microanalytical data. Reaction of 2-acetylpyridine thiosemicarbazone ($\mathbf{HL^B}$) and 2-pyridineformamide thiosemicarbazone ($\mathbf{HL^C}$) with $Ga(NO_3)_3 \cdot 9H_2O$ in 2:1 molar ratio in ethanol in the absence of a base produced complexes **1B** and **1C** in 69% and 55% yields, respectively. The gallium complexes of the ligands $\mathbf{HL^E}$–$\mathbf{HL^H}$ were prepared in methanol or ethanol and isolated as nitrates or in some cases as hexafluorophosphates ($\mathbf{HL^F}$ and $\mathbf{HL^H}$) by addition of excess NH_4PF_6 to the reaction mixture (60–91% yield).[24] Starting from $Fe(NO_3)_3 \cdot 9H_2O$ and the ligands $\mathbf{HL^B}$ and $\mathbf{HL^D}$–$\mathbf{HL^H}$ in methanol or ethanol, the iron(III) complexes were obtained in 66–76% yield (**2E** and **2F** were isolated as hexafluorophosphates).[24] The synthesis of the iron(III) complexes of $\mathbf{HL^A}$ and $\mathbf{HL^C}$ was carried out in the presence of *N*-methylmorpholine because this was found to improve their purity.

Characterization. The positive ion ESI mass spectra of all complexes showed very strong peaks due to $[M(L)_2]^+$ ions. A peak with m/z 145, attributed to $[PF_6]^-$, was registered in the negative ion mode for the hexafluorophosphates. In line with the UV–vis spectra of gallium(III) complexes of 2-acetylpyridine thiosemicarbazones,[24] **1A**–**1H** display a strong absorption band centered between 389 and 411 nm associated with intraligand transitions. This band is split and shifted to lower energies for **1D** (441 and 459 nm) and **1H** (451 and 469 nm). In the case of iron(III) complexes, charge transfer bands, intraligand transitions, and a d–d band centered between 829 and 977 nm attributed to the $^2T_{2g} \rightarrow {}^2T_{1g}$ transition for the d^5 low-spin system were observed.[33] The ^{1}H NMR spectrum of the ligand $\mathbf{HL^H}$ in DMSO-d_6 indicates the presence of only one isomeric form in solution. In contrast, two and three isomers were found for $\mathbf{HL^E}$ and $\mathbf{HL^F}$ in DMSO-d_6.[34,35] Interestingly, a second isomer with chemical shifts at 9.18 (NH), 8.58 (py), 7.86 (py), 7.45 (py), 6.78 (NH_2), and 3.28 ($N(CH_3)_2$) ppm (one pyridine proton signal overlaps with a signal of the main species) and ~20% content relative to the main isomer was found for $\mathbf{HL^G}$ in DMSO-d_6, in contrast to the data reported.[36] The signal intensity of the minor species decreases with time, implying its conversion into the main isomeric form of the ligand. In contrast to the metal-free ligands, the gallium(III) complexes show only one set of signals in the ^{1}H NMR spectra, due to the stabilization of the ligand configuration upon coordination to the metal and the equivalence of both ligands bound to gallium(III) in solution. The most remarkable difference between the ^{1}H NMR spectra of the metal-free ligands and those of the gallium(III) complexes is the absence of the N–H proton signals of the thiosemicarbazide moiety in the latter, indicating deprotonation of the ligands upon coordination.

X-ray Crystallography. X-ray diffraction quality single crystals of Triapine ($\mathbf{HL^D}$) were obtained by slow evaporation of the sodium bicarbonate neutralized mother liquor. The result of the X-ray diffraction study of $\mathbf{HL^D}$ is shown in Figure 1a, along with its gallium(III) (**1D**) and iron(III) (**2D**) complexes (Figure 1b and Figure 1c). Selected bond distances and angles are quoted in the caption of Figure 1. $\mathbf{HL^D}$ crystallized in the orthorhombic space group $Pna2_1$ with two crystallographically independent molecules in the asymmetric unit. Both adopt the *E*-isomeric form in terms of the nomenclature used for the conformations of α-N-heterocyclic thiosemicarbazones,[37] unlike the X-ray crystal structure of $\mathbf{HL^E}$ with a *Z* conformation (see Supporting Information Figure S2). In the gallium(III) and iron(III) complexes of Triapine (**1D** and **2D**) the coordination polyhedron approaches an octahedron, where the two ligands coordinate to the metal via the pyridine nitrogen atom and the nitrogen and sulfur donors of the thiosemicarbazide moiety. Deprotonation of both ligands is accompanied by an elongation of the carbon–sulfur bonds [**1D**, 1.735(6) and 1.743(7) Å; **2D**, 1.754(5) and 1.750(5) Å] compared to that in the metal-free ligand $\mathbf{HL^D}$ at 1.697(2) Å.

Electrochemistry. In phase I and phase II clinical trials, patients treated with Triapine developed methemoglobinemia,[15,38] a disorder characterized by the presence of a higher than normal level of methemoglobin (metHb) in the blood. This side effect was ascribed to the redox activity of the iron complex of Triapine, although its electrochemical

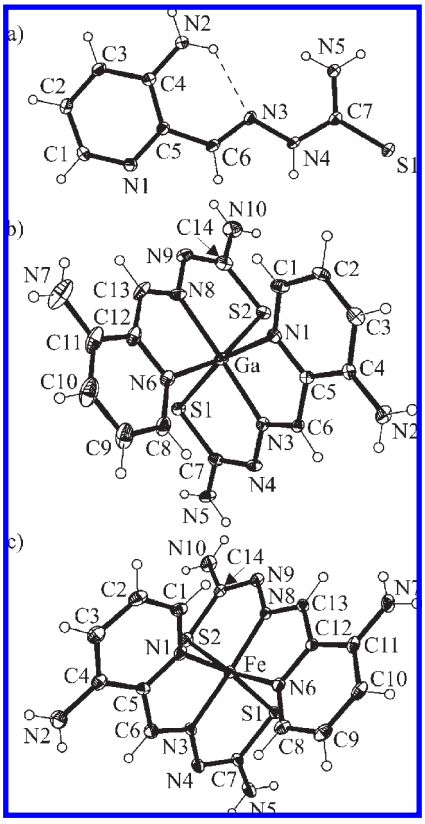

Figure 1. ORTEP plots of Triapine ($\mathbf{HL^D}$) (a), its gallium(III) complex (**1D**) (b), and iron(III) complex (**2D**) (c) with atom numbering schemes. The thermal ellipsoids are drawn at 50% ($\mathbf{HL^D}$ and **2D**) and 30% (**1D**) probability levels. Selected bond lengths (Å) and bond angles (deg) for $\mathbf{HL^D}$: C6−N3 1.283(2), N3−N4 1.384(2), N4−C7 1.344(2), C7−S1 1.697(2), C7−N5 1.325(3) Å; $\Theta_{(N2-C4-C5-C6)}$ 0.1(3)°, $\Theta_{(C5-C6-N3-N4)}$ 179.48(17)°, $\Theta_{(N3-N4-C7-S1)}$ 178.92(14)°. **1D**: Ga−N1 2.130(4), Ga−N6 2.110(5), Ga−N3 2.034(4), Ga−N8 2.040(5), Ga−S1 2.3722(14), Ga−S2 2.3563(16), C6−N3 1.301(6), C13−N8 1.279(7), N3−N4 1.362(6), N8−N9 1.379(7), N4−C7 1.339(7), N9−C14 1.332(8), C7−S1 1.735(6), C14−S2 1.743(7) Å; N1−Ga−N3 77.77(17)°, N6−Ga−N8 77.60(19)°, N3−Ga−S1 82.56(12)°, N8−Ga−S2 82.79(15)°. **2D**: Fe−N1 1.995(4), Fe−N6 2.011(4), Fe−N3 1.922(4), Fe−N8 1.925(4), Fe−S1 2.2302(13), Fe−S2 2.2171(14), C6−N3 1.299(6), C13−N8 1.299(6), N3−N4 1.379(5), N8−N9 1.379(5), N4−C7 1.318(6), N9−C14 1.323(6), C7−S1 1.754(5), C14−S2 1.750(5) Å; N1−Fe−N3 80.85(17)°, N6−Fe−N8 80.97(17)°, N3−Fe−S1 83.92(12)°, N8−Fe−S2 84.24(12)°.

Table 1. Electrochemical Data[a] for **1A**−**H** and **2A**−**H**

	Gallium Complexes		
	$E_{1/2}/{}^{I}L^{red}$	$E_{1/2}/{}^{II}L^{red}$	$E_p/{}^{III}L^{red}$
1A	−0.82	−1.10	−1.63[b,c]
1B	−0.93	−1.21	−1.80[b,c]
1C	−1.21	−1.46	−2.02[b,c]
1D	−0.94	−1.23	−1.78[b,c]
1E	−0.80	−1.09	−1.67[b,c]
1F	−0.92	−1.21	−1.77[b,c]
1G	−1.21	−1.47	−2.02[b,c]
1H	−0.93	−1.22	−1.78[b,c]
	Iron Complexes		
	$E_{1/2}/Fe^{III/II}$	$E_{1/2}/{}^{I}L^{red}$	$E_{1/2}/{}^{II}L^{red}$
2A	0.15	−1.44	−1.80[b]
2B	0.04	−1.58	−1.92[b]
2C	−0.21	−1.63	−2.02[b]
2D	0.01	−1.56	−1.92[b]
2E	0.18	−1.47	−1.78
2F	0.07	−1.60	−1.99[b,c]
2G	−0.22	−1.66	−2.04[b]
2H	0.03	−1.62	−1.92

[a] Potentials in V ± 0.01 vs NHE in 0.20 M [*n*-Bu_4N][BF_4]/DMSO. [b] For the irreversible waves, the E_p values are given. [c] Two-electron wave.

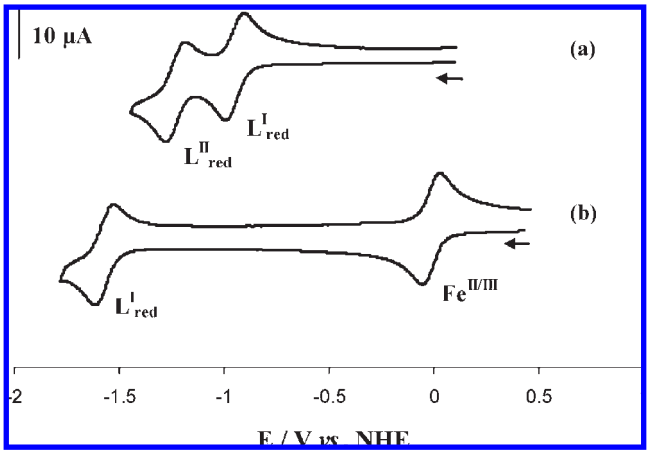

Figure 2. Cyclic voltammograms of complexes **1D** (a) and **2D** (b) in DMSO solution containing 0.20 M [*n*-Bu_4N][BF_4] at a scan rate of 0.20 V s^{-1} using a glassy carbon working electrode, displaying the ligand (L^{red}) and the Fe^{II}/Fe^{III} redox couple.

behavior was not studied. We investigated the electrochemical properties of all synthesized metal complexes by cyclic voltammetry, and the results are summarized in Table 1.

In 0.20 M [*n*-Bu_4N][BF_4]/DMSO solution all iron complexes display a reversible Fe^{III}/Fe^{II} redox couple between −0.21 and +0.18 V vs NHE (normal hydrogen electrode) depending on the ligand identity. A decrease of the redox potential in the order **2A** > **2B** > **2C** is in line with an increase of the electron donor properties of the corresponding ligands due to the presence of different substituents at the azomethine group (NH_2 > CH_3 > H). Likewise the electron donating properties of the amino group cause the redox potential shift of the iron(III) complex of Triapine (**2D**) at 0.01 V compared to the iron(III) complex of 2-formylpyridine thiosemicarbazone **2A** at +0.15 V vs NHE. Compared to **2A**−**D**, the reduction waves for the N^4-dimethyl substituted analogues **2E**−**H** are shifted by 10−30 mV to more positive potentials, in contrast to the expected negative shift because of the stronger electron donating properties of dimethylamine compared to ammonia [pK_a: dimethylamine, 10.73; ammonia, 9.25].[39] Besides the metal-centered reductions, the iron complexes display two ligand-centered reduction waves, the first ($^{I}L_{red}$) between −1.44 and −1.66 V (Figure 2) and the second ($^{II}L_{red}$) between −1.80 and −2.04 V vs NHE close to the solvent cutoff. For the corresponding gallium(III) complexes **1A**−**H** two reversible reductions ($^{I}L_{red}$ and $^{II}L_{red}$) from −0.80 to −1.21 and from −1.09 to −1.47 V, correspondingly, and an irreversible two-electron reduction ($^{III}L_{red}$) between −1.63 and −2.02 V vs NHE were observed. In comparison the ligand-centered redox couples $^{I}L_{red}$ and $^{II}L_{red}$ of the corresponding iron(III) complexes (which first are reduced to the iron(II) species) are negatively shifted by 400−700 mV. All the ligand-centered

redox processes can be attributed to the reduction of the C=N double bond(s) adjacent to the pyridine ring[40] (supplementary data on the electrochemical behavior of the complexes in DMSO and CH_3CN can be found in Supporting Information).

The influence of water on the iron redox potentials was studied by cyclic voltammetry measurements in H_2O/DMSO (7:3 v/v) mixtures with 0.2 M $NaClO_4$ as the supporting electrolyte. The low aqueous solubility of the complexes prevented the use of pure aqueous electrolyte solutions. The Fe^{III}/Fe^{II} redox couples remained reversible in H_2O/DMSO solution but were shifted by 10−50 mV to lower redox potentials, with exception of complexes **2D** (Figure S1) and **2H** which showed a positive shift by 30−40 mV.

Our data are in very good agreement with recently reported redox potentials for **2B** and **2F** in CH_3CN/H_2O (7:3) at 0.02 and 0.05 V vs NHE.[41] In cell-free assays Triapine was reported to enhance ascorbate oxidation, benzoate hydroxylation, and quenching of purified RR tyrosyl radical in the presence of iron salts.[27] In addition, EPR measurements showed that the iron(II) complex of Triapine is capable of reducing O_2 to reactive oxygen species (ROS).[25] The potential range and the reversibility of the redox couple of the iron complex **2D** in H_2O/DMSO solution provide further evidence that the complex is able to undergo redox cycling and produce ROS under physiological conditions. This conclusion is also valid for the other iron complexes studied in this work but probably to a lesser extent for complexes **2C** and **2G** with more negative potentials of the Fe^{III}/Fe^{II} redox couples at around −0.2 V vs NHE.

Cytotoxicity. The cytotoxic potency of the thiosemicarbazones and their corresponding gallium(III) and iron(III) complexes was measured in the human tumor cell lines 41M (ovarian carcinoma) and SK-BR-3 (mammary carcinoma) by means of the colorimetric MTT assay. Generally, the 41M cells were more sensitive to the compounds investigated in this study. The metal-free ligands and the corresponding metal complexes cover a broad range of activity, with IC_{50} values ranging from nanomolar to high micromolar concentrations, depending on the ligand substitutions and the metal ion (Table 2).

Structure−Activity Relationships of the Metal-Free Ligands. Specific structural modifications on the ligand were made to explore the following structure−activity relationships.

(i) Effect of Substituents at the Carbon Atom of the Azomethine Group. Substitution of the hydrogen atom in $\mathbf{HL^A}$ by a methyl group does not change the antiproliferative activity. However, the substitution of the hydrogen atom by a NH_2 group ($\mathbf{HL^C}$) results in about 2-fold decrease of cytotoxicity in both cell lines.

IC_{50} values for the ligands $\mathbf{HL^A}$ and $\mathbf{HL^B}$ were documented in the literature.[42] These are very similar, varying from 1 to 10 μM, depending on the cell line. The first 2-pyridineformamide thiosemicarbazones were synthesized 10 years ago with the aim of increasing aqueous solubility.[43] The first results on their cytotoxicity were reported only quite recently. In particular, $\mathbf{HL^C}$ tested in glioblastoma cell lines showed cytotoxicities in the micromolar concentration range (3.6−7.3 μM).[44] In the case of Triapine the reported IC_{50} values range from 0.2 to 3.0 μM.[27,45] However, because of the use of different cell lines and conditions, the impact of the structural changes in the ligands $\mathbf{HL^A}$−$\mathbf{HL^D}$ (all containing a terminal NH_2 group) remained vague. Our cytotoxicity data in both cell lines 41M and SK-BR-3 confirm that the antiproliferative activity of $\mathbf{HL^A}$ is very similar to that of $\mathbf{HL^B}$, whereas $\mathbf{HL^C}$ possesses a slightly lower cytotoxic potency (Table 2, Figure 3, Figure S5). Interestingly, $\mathbf{HL^D}$ shows IC_{50} values by a factor 10 lower than $\mathbf{HL^C}$, indicating that the effect of the second amino group is dependent on its position.

Table 2. Cytotoxicity of α-N-Heterocyclic Thiosemicarbazones ($\mathbf{HL^A}$−$\mathbf{HL^H}$) and Their Gallium(III) (**1A**−**H**) and Iron(III) Complexes (**2A**−**H**) in Two Human Cancer Cell Lines

	IC_{50} (μM)[a]	
compd	41M	SK-BR-3
	Ligands	
$\mathbf{HL^A}$	2.9 ± 0.6	3.2 ± 0.6
$\mathbf{HL^B}$	2.5 ± 0.3	3.6 ± 0.2
$\mathbf{HL^C}$	4.9 ± 0.04	5.6 ± 1.1
$\mathbf{HL^D}$, Triapine	0.45 ± 0.03	0.52 ± 0.08
$\mathbf{HL^E}$	0.0040 ± 0.0009	0.0098 ± 0.0011
$\mathbf{HL^G}$	0.32 ± 0.03	0.29 ± 0.01
$\mathbf{HL^H}$	0.21 ± 0.13	0.29 ± 0.08
	Ga(III) Complexes	
1A	1.5 ± 0.1	1.5 ± 0.5
1B	1.2 ± 0.1	1.0 ± 0.1
1C	3.4 ± 1.0	4.6 ± 1.1
1D	0.25 ± 0.05	0.35 ± 0.04
1E	0.0029 ± 0.0001	0.0050 ± 0.0009
1G	0.11 ± 0.05	0.12 ± 0.04
1H	0.074 ± 0.001	0.081 ± 0.006
	Fe(III) Complexes	
2A	2.7 ± 0.5	4.9 ± 0.5
2B	28 ± 12	>100
2C	>100	>100
2D	1.5 ± 0.5	1.7 ± 0.4
2E	0.11 ± 0.04	0.15 ± 0.05
2G	1.6 ± 0.7	1.5 ± 0.4
2H	5.2 ± 0.2	6.0 ± 0.9
$Ga(NO_3)_3$[b]	70 ± 4	>100
$Fe(NO_3)_3$[b]	>100	>100

[a] 50% inhibitory concentrations in 41M and SK-BR-3 cells after exposure for 96 h in the MTT assay. Values are the mean ± standard deviation obtained from at least three independent experiments. [b] Values taken from ref 24.

(ii) Dimethylation of the Terminal NH_2 Group. Terminal dimethylation enhances the activity of the thiosemicarbazones. However, the magnitude of this effect is strongly dependent on the other ligand substitutions. The strongest enhancement was observed when comparing $\mathbf{HL^A}$ with its dimethylated counterpart $\mathbf{HL^E}$. The N^4-dimethylation results in a 725-fold (41M) and 320-fold (SK-BR-3) increase of cytotoxicity (Table 2, Figure 3). The same trend but with distinctly smaller differences was observed for the two ligands containing a 2-pyridinecarboxamide moiety ($\mathbf{HL^C}$ vs $\mathbf{HL^G}$), with an increase of cytotoxicity by a factor of 15−20 as a result of dimethylation. The effect was found to be weakest for Triapine and its dimethylated derivative ($\mathbf{HL^D}$ vs $\mathbf{HL^H}$). In this case only a 2-fold increase of cytotoxicity was observed.

(iii) Effect of an Amino Group in Terminally Dimethylated Thiosemicarbazones. The cytotoxicity of the terminally dimethylated Triapine analogue $\mathbf{HL^H}$ is strongly diminished

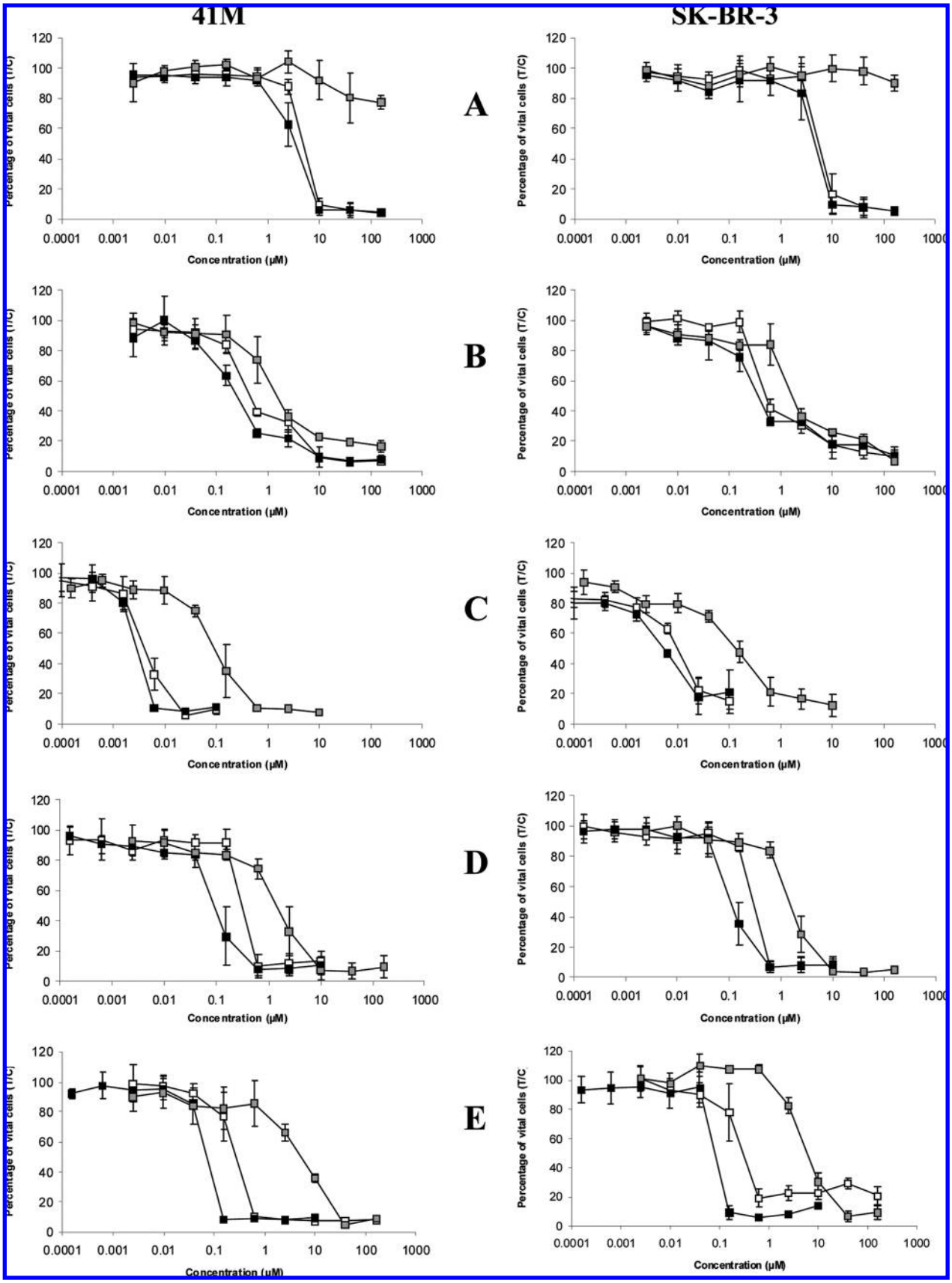

Figure 3. Concentration−effect curves of metal-free thiosemicarbazones (white symbols), their gallium(III) complexes (black symbols), and iron(III) complexes (gray symbols), obtained by the MTT assay in 41M cells (left panels) and SK-BR-3 cells (right panels): (A) $\mathbf{HL^C}$, **1C**, **2C**; (B) $\mathbf{HL^D}$, **1D**, **2D**; (C) $\mathbf{HL^E}$, **1E**, **2E**; (D) $\mathbf{HL^G}$, **1G**, **2G**; (E) $\mathbf{HL^H}$, **1H**, **2H**. Values are the mean ± standard deviation from at least three independent experiments.

compared to that of $\mathbf{HL^E}$, in which the amino group in position 3 of the pyridine heterocycle is absent. Thus, the addition of a NH_2 functionality to $\mathbf{HL^E}$ results in a 50- and 30-fold decrease of IC_{50} values in 41M and SK-BR-3 cells, respectively. Likewise the presence of the NH_2 group at the carbon atom of the azomethine bond in $\mathbf{HL^G}$ results in 30- to 80-fold decrease of cytotoxicity when compared to that of $\mathbf{HL^E}$. Together, these data suggest a critical role of the NH_2 group on the biological activity of terminally dimethylated α-N-heterocyclic thiosemicarbazones.

Thus, the most striking enhancement in cytotoxic activity (by a factor of ~300 to 700) was achieved by dimethylation of the terminal amino group of $\mathbf{HL^A}$. A similar effect was observed when the terminal NH_2 group of 2-acetylpyridine thiosemicarbazone was disubstituted.[41,46] On the other hand, our results demonstrate that the enhancement of cytotoxic potency by N^4-dimethylation is nearly annihilated when another NH_2 group is present ($\mathbf{HL^H}$, $\mathbf{HL^G}$). Hence, contrary to what has been assumed in the literature,[46] addition of the terminal methyl groups, while necessary, is not sufficient for the drastic enhancement in cytotoxic activity of these derivatives. Removal of any NH_2 functionality is also necessary.

Structure−Activity Relationships of the Metal Complexes. The effects of thiosemicarbazone complexation to gallium(III) and iron(III) are divergent (Table 2, Figure 3, Figure S5) and have been established by comparison of cytotoxicities of metal complexes and metal-free ligands. Generally, the iron(III) complexes show reduced cytotoxicity in comparison to that of the corresponding ligands. The effects vary from 3-fold to >28-fold increased IC_{50} values. In contrast to the iron(III) complexes, gallium(III) thiosemicarbazonates are 1.2−3.6 times more cytotoxic than the corresponding metal-free ligands.

In all previous studies the effect of Triapine complexation to iron has been determined by simple addition of iron salt to a solution of Triapine, assuming the formation of the desired complex. However, the applied procedure does not guarantee its formation. Given the conditions for complexation reactions are provided, mixtures of complexes with different metal-to-ligand stoichiometries and various coligands can be produced. This might explain why the reported effects of Triapine complexation to iron are divergent. On the one hand, an enhancement in cytotoxic activity was observed in murine leukemia cells.[26] On the other hand, a slight decrease was found in neuroblastoma cells,[27] whereas no difference was discernible in neuroephithelioma cells.[47] No marked differences were found between the cytotoxic potencies of iron(II) and iron(III) complexes, presumably because of spontaneous oxidation of iron(II) to iron(III) in cell culture medium.[26,47] Generally, the reported influence of the complexation of Triapine to iron is moderate, in contrast to classic iron chelating agents such as DFO (desferrioxamine), which result in iron complexes that are almost devoid of antiproliferative activity.[47] As the iron complex of Triapine retains reasonable activity, it is still conceivable that this complex is the active species. The latter is based on findings in cell-free assays showing that the iron(II) complex is able to react with dioxygen and generate reactive oxygen species (ROS) and that the preformed iron complex inhibits ribonucleotide reductase (RR) much more effectively than the metal-free ligand.[25]

In this study, the isolated iron(III) complex of Triapine (**2D**) is 3 times less cytotoxic in both cell lines than the metal-free ligand. Interestingly, this decrease in activity upon complexation with iron(III) is smaller than in the case of $\mathbf{HL^B}$, $\mathbf{HL^C}$, and $\mathbf{HL^E}$−$\mathbf{HL^H}$. Iron(III) complexes of these ligands are 5−30 times less cytotoxic than the uncomplexed ligands. Only complexation of $\mathbf{HL^A}$ to iron(III) did not result in a change in cytotoxicity. Taking into account the 1:2 stoichiometry of the iron thiosemicarbazonate complexes, the decrease in activity is even more pronounced. However, there is no clear correlation between the cytotoxic potencies of the iron(III) complexes and the uncomplexed ligands, suggesting that the binding strength to iron(III) or another factor has a modulating effect on cytotoxicity. The decreased cytotoxicity of the iron(III) complexes compared to that of the metal-free ligands can presumably be explained at least partially by the positive charge that impairs their ability to cross the cell membrane (see RR inhibition capacities below).

Table 3. Comparison of the RR Inhibitory Potency and Cytotoxicity of $\mathbf{HL^D}$, $\mathbf{HL^E}$, and Their Iron(III) Complexes **2D** and **2E** in HL60 Cells

	IC_{50} (μM)[a]	
compd	RR inhibition	cytotoxicity
$\mathbf{HL^D}$, Triapine	5.4 ± 2.4	0.27 ± 0.06
2D	53 ± 8.8	0.84 ± 0.05
$\mathbf{HL^E}$	0.80 ± 0.13	0.0068 ± 0.0022
2E	1.5 ± 0.8	0.11 ± 0.05

[a] 50% inhibitory concentrations in HL60 cells. RR inhibition was determined using ^{3}H-cytidine DNA incorporation assays after 4 h of drug incubation. Cytotoxicity was determined after exposure for 96 h by the MTT assay. Values are the mean ± standard deviations from at least three independent experiments.

We have previously noted an enhancement of antiproliferative activity of gallium(III) complexes in comparison to their corresponding ligands.[24] In this study this trend is preserved, with about 2-fold increase of cytotoxic activity compared to the respective metal-free ligands. These results suggest that the higher activity of the gallium(III) complexes is mainly due to the stoichiometric effect of the 1:2 gallium-to-ligand complexes.

Inhibition of Ribonucleotide Reductase. ^{3}H-Cytidine DNA incorporation assays were performed in HL60 cells after 4 h of drug incubation for $\mathbf{HL^D}$, $\mathbf{HL^E}$, **2D**, and **2E** in order to ascertain whether the differences in cytotoxicity induced by coordination to iron(III) and/or by terminal dimethylation are related to different capacities of inhibiting RR. As shown in Table 3, the RR inhibitory potential follows the same trends as observed in the cytotoxicity tests, but in detail some differences are obvious. The cytotoxicity data show only a small increase in the IC_{50} values after coordination of $\mathbf{HL^D}$ to iron(III) (**2D**), whereas the effect of coordination to iron(III) on RR inhibition is much more pronounced. The magnitudes of these effects are in reversed order for $\mathbf{HL^E}$ and **2E**. While the ability of **2E** to inhibit RR is only slightly decreased, the cytotoxicity of **2E** is reduced by a factor of 16 compared to the metal-free ligand $\mathbf{HL^E}$. Concerning the terminal dimethylation, the strong increase in cytotoxicity from $\mathbf{HL^D}$ to $\mathbf{HL^E}$ is not paralleled to the same extent by their ability to inhibit RR. Notably, in the IC_{50} range even small increases in drug concentration of the metal-free ligands induce strong effects on RR activity (Figure 4). In contrast, the iron complexes show a gradual increase of RR inhibition over a broad drug concentration range.

It should be noted that the RR inhibitory potential of Triapine ($\mathbf{HL^D}$) is well documented in the literature. In particular, in cell-free systems short-time treatment of

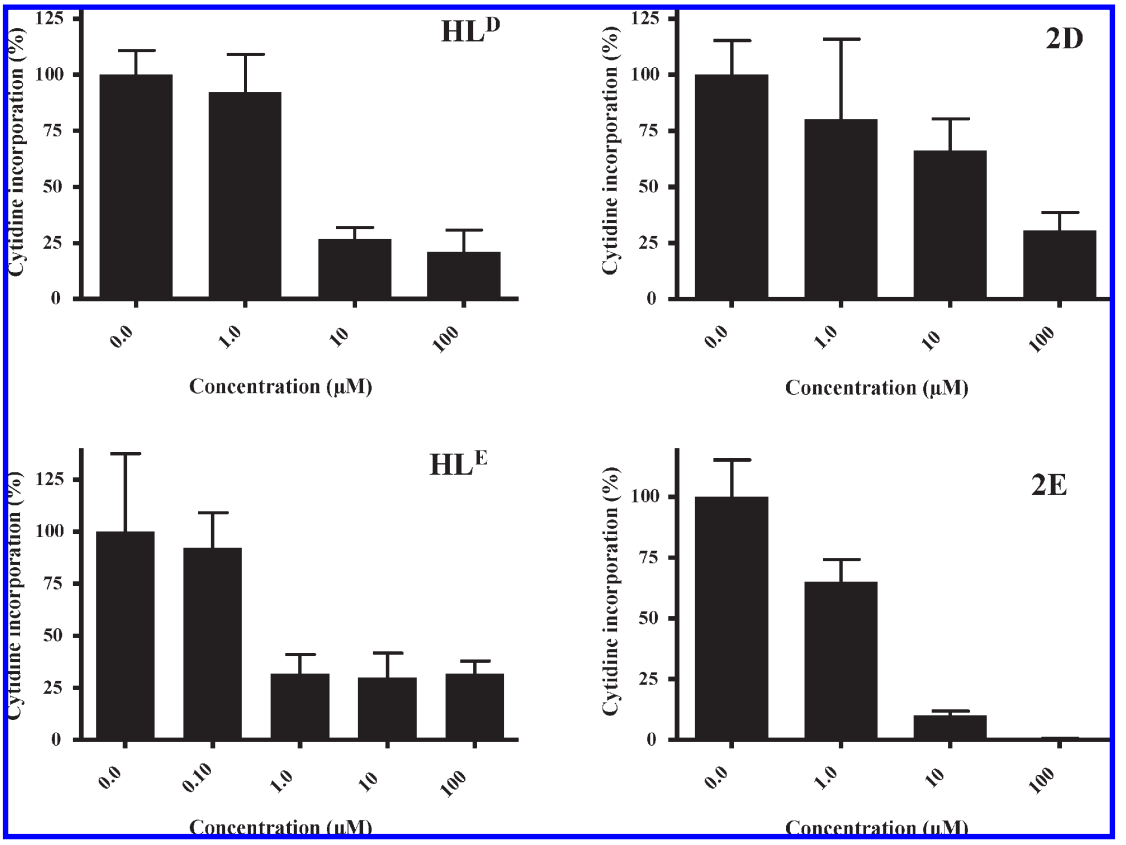

Figure 4. Inhibition of ribonucleotide reductase by HL^D (Triapine), HL^E, and their iron(III) complexes **2D** and **2E** as determined by ^{3}H-cytidine DNA incorporation assays in HL60 cells.

purified prokaryotic or mouse RR with Triapine resulted in reduced ^{3}H-cytidine incorporation into DNA.[25,26] In line with these data, EPR measurements of intact SK-MC neuroepithelioma cells after their treatment with 25 μM Triapine for 24 h showed a 39% quenching of the tyrosyl radical.[27] To our knowledge the RR inhibitory activity of the iron(III) complex of Triapine (**2D**) was so far determined exclusively under reducing conditions in cell-free systems.[25,26] Precomplexation of Triapine to iron was found to strongly enhance RR inhibition. This is in line with our previous report on enhanced tyrosyl radical quenching in isolated mouse R2 subunits by iron(III) N^4-dimethylated thiosemicarbazonates.[24] In the present study, the ability of HL^D, HL^E and their iron(III) complexes to inhibit RR was determined in living cells. Here, iron(III) complexes show a reduced RR inhibitory activity compared to the metal-free ligands, the difference being much more evident between HL^D and **2D**. The mechanisms underlying these effects are still not known. A possible explanation is the ionic nature and the reduced lipophilicity of the iron complex, which probably results in lower uptake into the cell. To clarify whether the differences observed between metal-free ligands and the respective iron complexes are based on reduced drug uptake or depend on other yet unknown mechanisms is a matter of ongoing investigations.

With regard to the impact of N^4-disubstitution on the RR inhibitory potency, only some in vitro tests with 5-hydroxy-2-formylpyridine thiosemicarbazones using purified RR have been reported so far.[48] In contrast to our data in living cells, those studies showed that dimethylation of the terminal amino group markedly decreased the RR inhibitory activity. However, taking into account that different assays for determination of RR inhibitory potencies were performed and that no cytotoxicity data were reported in the earlier study,[48] a direct comparison is not possible. Our data suggest that the enhancement in antiproliferative activity by terminal dimethylation cannot be solely dependent on RR inhibition and that other intracellular targets may be involved.

Conclusions

In this study we developed a novel straightforward three-step synthesis of Triapine, the most promising α-N-heterocyclic thiosemicarbazone for cancer therapy today. In addition, iron(III) and gallium(III) complexes of Triapine were prepared for the first time. The synthesis of 2-formylpyridine, 2-acetylpyridine, 2-pyridineformamide thiosemicarbazones, and their N^4-dimethylated analogues as well as the corresponding gallium(III) and iron(III) complexes allowed us to establish novel structure−cytotoxicity relationships. In particular, they revealed an increase of cytotoxicity by complexation of Triapine and related ligands to gallium(III), while coordination to iron(III) reduces their activity. Terminal nitrogen dimethylation was found to strongly enhance the cytotoxicity of metal-free ligands as well as their iron(III) and gallium(III) complexes. This is, however, not the case, when a NH_2 functionality is present anywhere at the thiosemicarbazone backbone. ^{3}H-Cytidine DNA incorporation assays showed that the increased cytotoxicity upon terminal dimethylation is only partly dependent on the ability of these compounds to inhibit RR, implying that other mechanisms are involved. Taken together, this study indicates the importance of detailed structure−activity relationship analyses for

the understanding of the molecular mechanisms underlying the anticancer activity of thiosemicarbazones and for the creation of more effective chemotherapeutics.

Experimental Section

All solvents and reagents were obtained from commercial suppliers and used without further purification. 2-Acetylpyridine N^4-dimethylthiosemicarbazone ($\mathbf{HL^F}$) and its gallium(III) (**1F**) and iron(III) complexes (**2F**) were prepared as previously reported.[24] 2-Formylpyridine thiosemicarbazone ($\mathbf{HL^A}$) was synthesized by refluxing 2-formylpyridine with thiosemicarbazide in EtOH/H_2O, 3:2, for 5 h, and 2-formylpyridine N^4-dimethylthiosemicarbazone ($\mathbf{HL^E}$) by refluxing 2-formylpyridine and N^4-dimethylthiosemicarbazide[49] in MeOH for 5 h (X-ray diffraction quality crystals of $\mathbf{HL^E}$ were obtained by recrystallization from methanol). 2-Acetylpyridine thiosemicarbazone ($\mathbf{HL^B}\cdot 0.5H_2O$) was obtained by refluxing 2-acetylypridine and thiosemicarbazide in EtOH for 5 h, followed by recrystallization in EtOH. The content of water was confirmed by thermogravimetric analysis. 2-Pyridineformamide thiosemicarbazone ($\mathbf{HL^C}$) was prepared following the literature protocol.[50] 2-Pyridineformamide N^4-dimethylthiosemicarbazone ($\mathbf{HL^G}$) was synthesized in a similar manner by using N^4-dimethylthiosemicarbazide instead of thiosemicarbazide, with a 76% yield, in comparison to 25% reported in the literature.[36] *tert*-Butyl (2-formylpyridin-3-yl)carbamate was obtained using *tert*-butyl (2-bromopyridin-3-yl)carbamate (see Supporting Information), *n*-butyllithium, and *N*-formylpiperidine.[32] The condensation reaction with thiosemicarbazide and deprotection were performed according to the published procedure.[29] Elemental analyses of prepared compounds were carried out on a Carlo Erba microanalyzer at the Microanalytical Laboratory of the University of Vienna and are within ±0.4% of the calculated values, confirming their ≥95% purity. Electrospray ionization mass spectrometry was carried out with a Bruker Esquire 3000 instrument (Bruker Daltonic, Bremen, Germany). Expected and experimental isotope distributions were compared. Infrared spectra were obtained from KBr pellets with a Perkin-Elmer FT-IR 2000 instrument (4000−400 cm^{-1}). UV−vis spectra were recorded on a Perkin-Elmer Lambda 650 UV−vis spectrophotometer using samples dissolved in methanol (900−210 nm). The iron(III) complexes were also measured on a Hewlett-Packard 8453 UV−vis spectrophotometer (1100−210 nm). The content of water in complexes **1C**, **2C**, and **2D** was verified by thermogravimetric analysis (TGA) with a Mettler Toledo TGA/SDTA851e apparatus, with a 3 °C/min heating rate under an air atmosphere. ^1H and ^{13}C one- and two-dimensional NMR spectra were recorded in DMSO-d_6, with a Bruker Avance III 500 MHz FT-NMR spectrometer. The residual ^1H and ^{13}C present in DMSO-d_6 were used as internal references. Abbreviations for NMR data are as follows: py = pyridine, $C_{q,py}$ = quaternary carbon of pyridine.

Electrochemistry. Cyclic voltammograms were measured in a three-electrode cell using a 2.0 mm diameter glassy carbon working electrode, a platinum auxiliary electrode, and an $Ag|Ag^+$ reference electrode containing 0.10 M $AgNO_3$. Measurements were performed at room temperature using an EG & G PARC 273A potentiostat/galvanostat. Deaeration of solutions was accomplished by passing a stream of argon through the solution for 5 min prior to the measurement and then maintaining a blanket atmosphere of argon over the solution during the measurement. The potentials were measured in 0.20 M [*n*-Bu_4N][BF_4]/DMSO, using [Fe(η^5-C_5H_5)$_2$] ($E_{1/2}$ = +0.68 V vs NHE)[51] as internal standard and are quoted relative to the normal hydrogen electrode (NHE). For cyclic voltammetry measurements in 0.20 M $NaClO_4$ DMSO/H_2O (3:7 v/v) solutions, a 2.0 mm diameter glassy carbon working electrode, a platinum auxiliary electrode, and an $Ag|Ag^+$ reference electrode containing 3.0 M NaCl were used.

Synthesis of Ligands and Metal Complexes. 3-Aminopyridine-2-carboxaldehyde-N^4-dimethylthiosemicarbazone ($\mathbf{HL^H}$). To *tert*-butyl (2-formylpyridin-3-yl)carbamate (147 mg, 0.66 mmol) and N^4-dimethylthiosemicarbazide (79 mg, 0.66 mmol) in ethanol (3 mL) and H_2O (1 mL) was added concentrated HCl (0.3 mL), and the mixture was stirred under reflux for 5 h. After the mixture was cooled to room temperature, 10% (w/w) aqueous $NaHCO_3$ (0.8 mL) was added and the mixture was stirred for further 30 min. The yellow hygroscopic $\mathbf{HL^H}\cdot$HCl was filtered off, washed with cold water, cold ethanol (−20 °C), and diethyl ether, and dried in vacuo. Yield: 130 mg (76%). ^1H NMR (500.10 MHz, DMSO-d_6): δ 12.00 (s, 1H, NH), 8.88 (s, 1H, HC=N), 8.15 (br s, 2H, NH_2), 8.03 (m, 1H, py), 7.69 (d, $^3J_{H,H}$ = 8.2 Hz, 1H, py), 7.57 (m, 1H, py), 3.35 (s, 6H, $N(CH_3)_2$). The $\mathbf{HL^H}\cdot$HCl salt (90 mg, 0.35 mmol) was dissolved in H_2O (4 mL) at 70 °C, and *N*-methylmorpholine (60 μL, 0.55 mmol) was added. The reaction mixture was cooled to room temperature and stirred for 1 h. The precipitate was filtered off, washed with H_2O, cold ethanol (−20 °C), and diethyl ether, and dried in vacuo and afterward over P_2O_5. Yield: 65 mg (84%). Anal. ($C_9H_{13}N_5S$) C, H, N, S. ^1H and ^{13}C NMR, IR, and UV−vis spectroscopy and mass spectrometry data for $\mathbf{HL^H}$ and all reported complexes can be found in Supporting Information.

[Bis(2-formylpyridinethiosemicarbazonato)-*N*,*N*,*S*-gallium(III)] Nitrate, [Ga($\mathbf{L^A}$)$_2$]$NO_3\cdot 0.5CH_3OH$ (1A). To 2-formylpyridine thiosemicarbazone ($\mathbf{HL^A}$) (140 mg, 0.78 mmol) and $NaOCH_3$ (63 mg, 1.17 mmol) in dry methanol (14 mL) at 70 °C under an argon atmosphere, gallium(III) nitrate nonahydrate (162 mg, 0.39 mmol) was added, and the mixture was stirred at 70 °C for 3 h, then cooled to room temperature and filtered from undissolved impurities. The clear solution was allowed to stand at +4 °C for 3 days, and the crystals formed were filtered off, washed with cold methanol (−20 °C), and dried in vacuo. Yield: 54 mg (27%). Anal. ($C_{14}H_{14}GaN_9O_3S_2\cdot 0.5CH_3OH$) C, H, N.

[Bis(2-acetylpyridinethiosemicarbazonato)-*N*,*N*,*S*-gallium(III)] Nitrate, [Ga($\mathbf{L^B}$)$_2$]NO_3 (1B). To 2-acetylpyridine thiosemicarbazone ($\mathbf{HL^B}$) (200 mg, 1.03 mmol) in ethanol (5 mL) at 70 °C, gallium(III) nitrate nonahydrate (217 mg, 0.52 mmol) in ethanol (2 mL) was added, and the solution was stirred at 50 °C for 2 h. The reaction mixture was cooled to room temperature and allowed to stand at +4 °C for 4 h. The yellow precipitate was filtered off, washed with cold ethanol (−20 °C) and diethyl ether, and dried in vacuo. Yield: 185 mg (69%). Anal. ($C_{16}H_{18}GaN_9O_3S_2$) C, H, N, S.

[Bis(2-pyridineformamidethiosemicarbazonato)-*N*,*N*,*S*-gallium(III)] Nitrate, [Ga($\mathbf{L^C}$)$_2$]$NO_3\cdot 0.5H_2O$ (1C). To 2-pyridineformamide thiosemicarbazone ($\mathbf{HL^C}$) (200 mg, 1.02 mmol) in ethanol (20 mL) at 70 °C, gallium(III) nitrate nonahydrate (214 mg, 0.51 mmol) in ethanol (2.5 mL) was added, and the mixture was stirred at the same temperature for 1 h. The yellow solid was separated from the hot solution by filtration, washed with ethanol, dried in vacuo at 50 °C and then over P_2O_5. Yield: 148 mg (55%). Anal. ($C_{14}H_{16}GaN_{11}O_3S_2\cdot 0.5H_2O$) C, H, N, S.

[Bis(3-aminopyridine-2-carboxaldehydethiosemicarbazonato)-*N*,*N*,*S*-gallium(III)] Nitrate, [Ga($\mathbf{L^D}$)$_2$]$NO_3\cdot 0.15CH_3OH$ (1D). To a suspension of 3-aminopyridine-2-carboxaldehyde thiosemicarbazone ($\mathbf{HL^D}$) (150 mg, 0.77 mmol) in methanol (10 mL) and triethylamine (112 μL, 0.81 mmol) at 50 °C, gallium(III) nitrate nonahydrate (166 mg, 0.40 mmol) in methanol (2.5 mL) was added, and the mixture was stirred for 20 min at 50 °C and 2.5 h at room temperature. The bright-orange precipitate formed was filtered off, washed with cold methanol (−20 °C), and dried in vacuo and afterward over P_2O_5. Yield: 144 mg (72%). Anal. ($C_{14}H_{16}GaN_{11}O_3S_2\cdot 0.15CH_3OH$) C, H, N, S. Crystals suitable for X-ray data collection were obtained by slow evaporation of an ethanolic solution of **1D**.

[Bis(2-formylpyridine-N^4-dimethylthiosemicarbazonato)-*N*,*N*,*S*-gallium(III)] Hexafluorophosphate, [Ga($\mathbf{L^E}$)$_2$]PF_6 (1E). To 2-formylpyridine N^4-dimethylthiosemicarbazone ($\mathbf{HL^E}$) (87 mg, 0.42 mmol) in methanol (6 mL) at 40 °C, gallium(III) nitrate

nonahydrate (87 mg, 0.21 mmol) in methanol (2 mL) was added, and the mixture was stirred at room temperature for 3 h. Addition of ammonium hexafluorophosphate (100 mg, 0.61 mmol) to the reaction mixture led to the formation of a yellow solid which was filtered off, washed with methanol, and dried in vacuo. Yield: 92 mg (70%). Anal. ($C_{18}H_{22}F_6GaN_8PS_2$) C, H, N, S.

[Bis(2-pyridineformamide-N^4-dimethylthiosemicarbazonato)-*N*,*N*,*S*-gallium(III)] Nitrate [Ga(L^G)$_2$]NO_3, (1G). To 2-pyridineformamide N^4-dimethylthiosemicarbazone (HL^G) (400 mg, 1.79 mmol) in ethanol (20 mL) at 70 °C, gallium(III) nitrate nonahydrate (375 mg, 0.90 mmol) in ethanol (5 mL) was added, and the mixture was stirred at the same temperature for 2 h. The yellow-orange solid was separated from the hot solution by filtration, washed with ethanol, and dried in vacuo. Yield: 380 mg (74%). Anal. ($C_{18}H_{24}GaN_{11}O_3S_2$) C, H, N, S.

[Bis(3-aminopyridine-2-carboxaldehyde-N^4-dimethylthiosemicarbazonato)-*N*,*N*,*S*-gallium(III)] Hexafluorophosphate, [Ga(L^H)$_2$]PF_6 (1H). To a suspension of 3-aminopyridine-2-carboxaldehyde N^4-dimethylthiosemicarbazone hydrochloride ($HL^H \cdot HCl$) (150 mg, 0.58 mmol) in ethanol (15 mL), gallium(III) nitrate nonahydrate (130 mg, 0.31 mmol) in ethanol (3 mL) was added and the mixture was stirred for 1.5 h at room temperature. Subsequently a solution of ammonium hexafluorophosphate (200 mg, 1.23 mmol) in ethanol (2 mL) was added. After 2 h the orange precipitate was filtered off, washed with cold ethanol (−20 °C), and dried in vacuo. Yield: 114 mg (60%). Anal. ($C_{18}H_{24}F_6GaN_{10}PS_2$) C, H, N, S.

[Bis(2-formylpyridinethiosemicarbazonato)-*N*,*N*,*S*-iron(III)] Nitrate, [Fe(L^A)$_2$]NO_3 (2A). To 2-formylpyridine thiosemicarbazone (HL^A) (200 mg, 1.11 mmol) and *N*-methylmorpholine (120 μL, 1.09 mmol) in methanol (20 mL) at 70 °C, iron(III) nitrate nonahydrate (222 mg, 0.55 mmol) in methanol (2 mL) was added dropwise, and the reaction mixture was stirred for 3 h at 70 °C. After the mixture was cooled to room temperature, about one half of the solvent was removed under reduced pressure and the reaction mixture was allowed to stand at +4 °C overnight. The black crystalline product was filtered off, washed with cold methanol, and dried in vacuo and afterward over P_2O_5. Yield: 195 mg (74%). Anal. ($C_{14}H_{14}FeN_9O_3S_2$) C, H, N, S.

[Bis(2-acetylpyridinethiosemicarbazonato)-*N*,*N*,*S*-iron(III)] Nitrate, [Fe(L^B)$_2$]NO_3 (2B). To 2-acetylpyridine thiosemicarbazone (HL^B) (200 mg, 1.03 mmol) in methanol (10 mL) at room temperature, iron(III) nitrate nonahydrate (208 mg, 0.51 mmol) in methanol (2 mL) was added dropwise, and the reaction mixture was stirred for 3 h. The black product formed was filtered off, washed with methanol, and dried in vacuo and then over P_2O_5. Yield: 198 mg (74%). Anal. ($C_{16}H_{18}FeN_9O_3S_2$) C, H, N, S.

[Bis(2-pyridineformamidethiosemicarbazonato)-*N*,*N*,*S*-iron(III)] Nitrate, [Fe(L^C)$_2$]$NO_3 \cdot 1.5H_2O$ (2C). To 2-pyridineformamide thiosemicarbazone (HL^C) (200 mg, 1.02 mmol) and *N*-methylmorpholine (111 μL, 1.01 mmol) in methanol (10 mL) at 50 °C, iron(III) nitrate nonahydrate (205 mg, 0.51 mmol) in methanol (2 mL) was added, and the mixture was stirred at 50 °C for 2 h. After the mixture was cooled to room temperature, about one half of the solvent was removed under reduced pressure and the reaction mixture was allowed to stand at +4 °C overnight. The black crystals were filtered off, washed with cold methanol, and dried in vacuo. Yield: 213 mg (78%). Anal. ($C_{14}H_{16}FeN_{11}O_3S_2 \cdot 1.5H_2O$) C, H, N, S.

[Bis(3-aminopyridine-2-carboxaldehydethiosemicarbazonato)-*N*,*N*,*S*-iron(III)] nitrate, [Fe(L^D)$_2$]$NO_3 \cdot H_2O$ (2D). To a suspension of 3-aminopyridine-2-carboxaldehyde thiosemicarbazone (HL^D) (150 mg, 0.77 mmol) in ethanol (24 mL) at 50 °C, iron(III) nitrate nonahydrate (157 mg, 0.39 mmol) in ethanol (2 mL) was added dropwise, and the mixture was stirred for 10 min at 50 °C and 3 h at room temperature. The black-green precipitate was filtered off, washed with cold ethanol (−20 °C) and diethyl ether, and dried in vacuo and afterward over P_2O_5. Yield: 132 mg (66%). Anal. ($C_{14}H_{16}FeN_{11}O_3S_2 \cdot H_2O$) C, H, N, S. Crystals suitable for X-ray data collection were obtained by slow evaporation of a methanolic solution of **2D**.

[Bis(2-formylpyridine-N^4-dimethylthiosemicarbazonato)-*N*,*N*,*S*-iron(III)] Hexafluorophosphate, [Fe(L^E)$_2$]PF_6 (2E). To 2-formylpyridine N^4-dimethylthiosemicarbazone (HL^E) (70 mg, 0.34 mmol) dissolved in ethanol (7 mL) at 40 °C, iron(III) nitrate nonahydrate (68 mg, 0.17 mmol) in ethanol (2 mL) was added, and the mixture was stirred at room temperature for 1.5 h. After addition of ammonium hexafluorophosphate (90 mg, 0.55 mmol) the reaction mixture was stirred further for 1 h. The solid was filtered off, washed three times with cold ethanol (−20 °C), and dried in vacuo and then over P_2O_5. Yield: 79 mg (76%). Anal. ($C_{18}H_{22}F_6FeN_8PS_2$) C, H, N, S.

[Bis(2-pyridineformamide-N^4-dimethylthiosemicarbazonato)-*N*,*N*,*S*-iron(III)] Nitrate, [Fe(L^G)$_2$]NO_3 (2G). To 2-pyridineformamide N^4-dimethylthiosemicarbazone (HL^G) (400 mg, 1.79 mmol) in methanol (30 mL) at 50 °C, iron(III) nitrate nonahydrate (362 mg, 0.90 mmol) in methanol (3 mL) was added, and the mixture was stirred at the same temperature for 2 h. After the mixture was cooled to room temperature about one half of the solvent was removed under reduced pressure and the reaction mixture was allowed to stand at +4 °C overnight. The precipitate was filtered off, washed with ethanol, and dried in vacuo at 50 °C. Yield: 340 mg (68%). Anal. ($C_{18}H_{24}FeN_{11}O_3S_2$) C, H, N, S.

[Bis(3-aminopyridine-2-carboxaldehyde-N^4-dimethylthiosemicarbazonato)-*N*,*N*,*S*-iron(III)] nitrate, [Fe(L^H)$_2$]NO_3 (2H). To a suspension of 3-aminopyridine-2-carboxaldehyde N^4-dimethylthiosemicarbazone hydrochloride ($HL^H \cdot HCl$) (120 mg, 0.46 mmol) in ethanol (12 mL), iron(III) nitrate nonahydrate (100 mg, 0.25 mmol) in ethanol (1 mL) was added dropwise, and the mixture was stirred for 3 h at room temperature. The brown precipitate was filtered off, washed with cold ethanol (−20 °C) and diethyl ether, and dried in vacuo at 50 °C and then over P_2O_5. Yield: 95 mg (73%). Anal. ($C_{18}H_{24}FeN_{11}O_3S_2$) C, H, N, S.

Crystallographic Structure Determination. X-ray diffraction measurements were performed on a Bruker X8 APEX II CCD diffractometer. Crystal data, data collection parameters, and structure refinement details for HL^D, HL^E, **1D**, and **2D** are given in Tables S1 and S2. The structures were solved by direct methods and refined by full-matrix least-squares techniques. Non-hydrogen atoms were refined with anisotropic displacement parameters. H atoms were placed at calculated positions and refined as riding atoms in the subsequent least-squares model refinements. The isotropic thermal parameters were estimated to be 1.2 times the values of the equivalent isotropic thermal parameters of the atoms to which hydrogens were bonded. The following computer programs were used: structure solution, SHELXS-97;[52] refinement, SHELXL-97;[53] molecular diagrams, ORTEP;[54] computer, Pentium IV; scattering factors.[55] Crystallographic data have been deposited at the Cambridge Crystallographic Data Center with numbers CCDC729370-729373. Copies of data can be obtained, free of charge, on application to CCDC, 12 Union Road, Cambridge CB2 1EZ, U.K. (deposit@ccdc.com.ac.uk).

Cell Lines and Culture Conditions. Human 41 M (ovarian carcinoma) and SK-BR-3 (mammary carcinoma) cells were kindly provided by Lloyd R. Kelland (CRC Centre for Cancer Therapeutics, Institute of Cancer Research, Sutton, U.K.) and Evelyn Dittrich (Department of Medicine I, Medical University of Vienna, Austria), respectively. Cells were grown in 75 cm^2 culture flasks (Iwaki/Asahi Technoglass, Gyouda, Japan) as adherent monolayer cultures in minimal essential medium (MEM) supplemented with 10% heat-inactivated fetal bovine serum, 1 mM sodium pyruvate, 4 mM L-glutamine, and 1% nonessential amino acids (100×) (all purchased from Sigma-Aldrich, Vienna, Austria). Cultures were maintained at 37 °C in a humidified atmosphere containing 5% CO_2.

Cytotoxicity Tests in Cancer Cell Lines. Antiproliferative effects were determined by means of a colorimetric microculture assay (MTT assay, MTT = 3-(4,5-dimethyl-2-thiazolyl)-2,5-diphenyl-2*H*-tetrazolium bromide). Cells were harvested from culture flasks by trypsinization and seeded in 100 μL aliquots into 96-well microculture plates (Iwaki/Asahi Technoglass, Gyouda, Japan) in densities of 4×10^3 cells/well, in order to ensure exponential growth of untreated controls throughout the experiment. After a 24 h preincubation, dilutions of the test compounds in 100 μL/well complete culture medium were added. Because of low aqueous solubility, the test compounds were dissolved in DMSO first and then serially diluted in complete culture medium such that the effective DMSO content did not exceed 0.5%. After exposure for 96 h, all media were replaced by 100 μL/well RPMI 1640 medium (supplemented with 10% heat-inactivated fetal bovine serum and 2 mM L-glutamine) plus 20 μL/well MTT solution in phosphate-buffered saline (5 mg/mL). After incubation for 4 h, the medium/MTT mixtures were removed, and the formazan crystals formed by vital cells were dissolved in 150 μL of DMSO per well. Optical densities at 550 nm were measured with a microplate reader (Tecan Spectra Classic), using a reference wavelength of 690 nm to correct for unspecific absorption. The quantity of vital cells was expressed in terms of T/C values by comparison to untreated control microcultures, and 50% inhibitory concentrations (IC_{50}) were calculated from concentration−effect curves by interpolation. Evaluation is based on mean values from at least three independent experiments, each comprising at least three microcultures per concentration level.

Ribonucleotide Reductase Inhibition. To compare the RR inhibitory potential of $\mathbf{HL^D}$ and $\mathbf{HL^E}$ with that of their corresponding iron complexes **2D** and **2E**, ^{3}H-cytidine incorporation assays were performed.[56] For this purpose, exponentially growing HL60 cells (5×10^6) were incubated with the test substances for 4 h. After the incubation period, the cells were pulsed with ^{3}H-cytidine (0.3125 μCi, 5 nM) for 1 h at 37 °C. Then cells were collected and washed with PBS. For cell lysis, the cell pellets were resuspended in a lysis buffer containing 10 mM EDTA, 50 mM Tris (pH 8.0), and 0.5% sodium lauryl sarcosine and frozen at −20 °C. For DNA extraction, the cell lysate was incubated with 20 units RNAse at 37 °C for 1 h followed by 24 h of treatment with 150 μg of proteinase K. Subsequently DNA was extracted using standard procedures. After precipitation with ethanol, DNA was resuspended in water, DNA content was measured, and radioactivity was determined.[57]

Acknowledgment. The authors are indebted to the FFG (Austrian Research Promotion Agency, Project No. 811591), to the Austrian Council for Research and Technology Development, and to COST (European Cooperation in the Field of Scientific and Technical Research) for financial support. We also thank Florian Biba and Anatoly Dobrov for thermogravimetric and mass spectrometry measurements, respectively.

Supporting Information Available: Literature reaction pathways to Triapine, cyclic voltammogram of the iron(III) complex **2D** in H_2O/DMSO, supplementary data on the electrochemical behavior of the complexes in DMSO and CH_3CN, spectroscopic (^{1}H and ^{13}C NMR, IR, and UV−vis) and microanalytical data for all novel compounds, crystallographic data in CIF format, details of X-ray data collection and refinement, results of X-ray diffraction studies of $\mathbf{HL^E}$, packing diagrams of $\mathbf{HL^D}$, $\mathbf{HL^E}$, **1D**, and concentration−effect curves of $\mathbf{HL^A}$, **1A**, **2A**, $\mathbf{HL^B}$, **1B**, and **2B**. This material is available free of charge via the Internet at http://pubs.acs.org.

References

(1) Casas, J. S.; Garcia-Tasende, M. S.; Sordo, J. Main group metal complexes of semicarbazones and thiosemicarbazones. A structural review. *Coord. Chem. Rev.* **2000**, *209*, 197–261.
(2) Lobana, T. S.; Rekha; Butcher, R. J.; Castineiras, A.; Bermejo, E.; Bharatam, P. V. Bonding trends of thiosemicarbazones in mononuclear and dinuclear copper(I) complexes: syntheses, structures, and theoretical aspects. *Inorg. Chem.* **2006**, *45*, 1535–1542.
(3) Barbazan, P.; Carballo, R.; Casas, J. S.; Garcia-Martinez, E.; Pereiras-Gabian, G.; Sanchez, A.; Vazquez-Lopez, E. M. Synthesis and characterization of new trimeric rhenium(I) complexes. The influence of steric factors on the size of pyrazolonaterhenium(I) metallomacrocycles. *Inorg. Chem.* **2006**, *45*, 7323–7330.
(4) Pedrido, R.; Romero, M. J.; Bermejo, M. R.; Gonzalez-Noya, A. M.; Garcia-Lema, I.; Zaragoza, G. Metal-catalyzed oxidation processes in thiosemicarbazones: new complexes with the ligand *N*-{2-([4-*N*-ethylthiosemicarbazone]-methyl)phenyl}-*p*-toluenesulfonamide. *Chem.—Eur. J.* **2008**, *14*, 500–512.
(5) West, D. X.; Padhye, S. B.; Sonawane, P. B. Structural and physical correlations in the biological properties of transition metal heterocyclic thiosemicarbazone and *S*-alkyl dithiocarbazate complexes. *Struct. Bonding (Berlin)* **1991**, *76*, 1–50.
(6) Bonnitcha, P. D.; Vavere, A. L.; Lewis, J. S.; Dilworth, J. R. In vitro and in vivo evaluation of bifunctional bisthiosemicarbazone ^{64}Cu-complexes for the positron emission tomography imaging of hypoxia. *J. Med. Chem.* **2008**, *51*, 2985–2991.
(7) Brockman, R. W.; Thomson, J. R.; Bell, M. J.; Skipper, H. E. Observations on the antileukemic activity of pyridine-2-carboxaldehyde thiosemicarbazone and thiocarbohydrazone. *Cancer Res.* **1956**, *16*, 167–170.
(8) French, F. A.; Blanz, E. J., Jr. The carcinostatic activity of thiosemicarbazones of formyl heteroaromatic compounds. III. Primary correlation. *J. Med. Chem.* **1966**, *9*, 585–589.
(9) DeConti, R. C.; Toftness, B. R.; Agrawal, K. C.; Tomchick, R.; Mead, J. A. R.; Bertino, J. R.; Sartorelli, A. C.; Creasey, W. A. Clinical and pharmacological studies with 5-hydroxy-2-formylpyridine thiosemicarbazone. *Cancer Res.* **1972**, *32*, 1455–1462.
(10) Krakoff, I. H.; Etcubanas, E.; Tan, C.; Mayer, K.; Bethune, V.; Burchenal, J. H. Clinical trial of 5-hydroxypicolinaldehyde thiosemicarbazone (5-HP; NSC-107392), with special reference to its iron-chelating properties. *Cancer Chemother. Rep.* **1974**, *58*, 207–212.
(11) Yu, Y.; Wong, J.; Lovejoy, D. B.; Kalinowski, D. S.; Richardson, D. R. Chelators at the cancer coalface: desferrioxamine to triapine and beyond. *Clin. Cancer Res.* **2006**, *12*, 6876–6883.
(12) Ma, B.; Goh, B. C.; Tan, E. H.; Lam, K. C.; Soo, R.; Leong, S. S.; Wang, L. Z.; Mo, F.; Chan, A. T. C.; Zee, B.; Mok, T. A multicenter phase II trial of 3-aminopyridine-2-carboxaldehyde thiosemicarbazone (3-AP, Triapine) and gemcitabine in advanced non-small-cell lung cancer with pharmacokinetic evaluation using peripheral blood mononuclear cells. *Invest. New Drugs* **2008**, *26*, 169–173.
(13) Karp, J. E.; Giles, F. J.; Gojo, I.; Morris, L.; Greer, J.; Johnson, B.; Thein, M.; Sznol, M.; Low, J. A phase I study of the novel ribonucleotide reductase inhibitor 3-aminopyridine-2-carboxaldehyde thiosemicarbazone (3-AP, Triapine) in combination with the nucleoside analog fludarabine for patients with refractory acute leukemias and aggressive myeloproliferative disorders. *Leuk. Res.* **2008**, *32*, 71–77.
(14) Mackenzie, M. J.; Saltman, D.; Hirte, H.; Low, J.; Johnson, C.; Pond, G.; Moore, M. J. A Phase II study of 3-aminopyridine-2-carboxaldehyde thiosemicarbazone (3-AP) and gemcitabine in advanced pancreatic carcinoma. A trial of the Princess Margaret Hospital Phase II consortium. *Invest. New Drugs* **2007**, *25*, 553–558.
(15) Knox, J. J.; Hotte, S. J.; Kollmannsberger, C.; Winquist, E.; Fisher, B.; Eisenhauer, E. A. Phase II study of Triapine in patients with metastatic renal cell carcinoma: a trial of the National Cancer Institute of Canada Clinical Trials Group (NCIC IND.161). *Invest. New Drugs* **2007**, *25*, 471–477.
(16) Moore, E. C.; Zedeck, M. S.; Agrawal, K. C.; Sartorelli, A. C. Inhibition of ribonucleoside diphosphate reductase by 1-formylisoquinoline thiosemicarbazone and related compounds. *Biochemistry* **1970**, *9*, 4492–4498.
(17) French, F. A.; Blanz, E. J., Jr.; Shaddix, S. C.; Brockman, R. W. α-(*N*)-Formylheteroaromatic thiosemicarbazones. Inhibition of tumor-derived ribunucleoside diphosphate reductase and correlation with in vivo antitumor activity. *J. Med. Chem.* **1974**, *17*, 172–181.
(18) Moore, E. C.; Sartorelli, A. C. Inhibition of ribonucleotide reductase by α-(N)-heterocyclic carboxaldehyde thiosemicarbazones. *Pharmacol. Ther.* **1984**, *24*, 439–447.
(19) Liu, M.-C.; Lin, T.-S.; Sartorelli, A. C. Chemical and biological properties of cytotoxic α-(N)-heterocyclic carboxaldehyde thiosemicarbazones. *Prog. Med. Chem.* **1995**, *32*, 1–35.
(20) Shao, J.; Zhou, B.; Chu, B.; Yen, Y. Ribonucleotide reductase inhibitors and future drug design. *Curr. Cancer Drug Targets* **2006**, *6*, 409–431.

(21) Kolberg, M.; Strand, K. R.; Graff, P.; Andersson, K. K. Structure, function, and mechanism of ribonucleotide reductases. *Biochim. Biophys. Acta* **2004**, *1699*, 1–34.
(22) Tanaka, H.; Arakawa, H.; Yamaguchi, T.; Shlralsh, K.; Fukuda, S.; Matsui, K.; Take, Y.; Nakamura, Y. A ribonucleotide reductase gene involved in a p53-dependent cell-cycle checkpoint for DNA damage. *Nature* **2000**, *404*, 42–49.
(23) Nakano, K.; Balint, E.; Ashcroft, M.; Vousden, K. H. A ribonucleotide reductase gene is a transcriptional target of p53 and p73. *Oncogene* **2000**, *19*, 4283–4289.
(24) Kowol, C. R.; Berger, R.; Eichinger, R.; Roller, A.; Jakupec, M. A.; Schmidt, P. P.; Arion, V. B.; Keppler, B. K. Gallium(III) and iron(III) complexes of α-N-heterocyclic thiosemicarbazones: synthesis, characterization, cytotoxicity, and interaction with ribonucleotide reductase. *J. Med. Chem.* **2007**, *50*, 1254–1265.
(25) Shao, J.; Zhou, B.; Di Bilio, A. J.; Zhu, L.; Wang, T.; Qi, C.; Shih, J.; Yen, Y. A ferrous-triapine complex mediates formation of reactive oxygen species that inactivate human ribonucleotide reductase. *Mol. Cancer Ther.* **2006**, *5*, 586–592.
(26) Finch, R. A.; Liu, M.-C.; Cory, A. H.; Cory, J. G.; Sartorelli, A. C. Triapine (3-aminopyridine-2-carboxaldehyde thiosemicarbazone; 3-AP). An inhibitor of ribonucleotide reductase with antineoplastic activity. *Adv. Enzyme Regul.* **1999**, *39*, 3–12.
(27) Chaston, T. B.; Lovejoy, D. B.; Watts, R. N.; Richardson, D. R. Examination of the antiproliferative activity of iron chelators: multiple cellular targets and the different mechanism of action of triapine compared with desferrioxamine and the potent pyridoxal isonicotinoyl hydrazone analogue 311. *Clin. Cancer Res.* **2003**, *9*, 402–414.
(28) Wang, Y.; Liu, M.-C.; Lin, T.-S.; Sartorelli, A. C. Synthesis and antitumor activity of 3- and 5-hydroxy-4-methylpyridine-2-carboxaldehyde thiosemicarbazones. *J. Med. Chem.* **1992**, *35*, 3667–3671.
(29) Niu, C.; Li, J.; Doyle, T. W.; Chen, S.-H. Synthesis of 3-amino-2-pyridinecarboxaldehyde thiosemicarbazone (3-AP). *Tetrahedron* **1998**, *54*, 6311–6318.
(30) Li, J.; Zheng, L.-M.; King, I.; Doyle, T. W.; Chen, S.-H. Syntheses and antitumor activities of potent inhibitors of ribonucleotide reductase: 3-amino-4-methylpyridine-2-carboxaldehyde-thiosemicarbazone (3-AMP), 3-amino-pyridine-2-carboxaldehyde-thiosemicarbazone (3-AP) and its water-soluble prodrugs. *Curr. Med. Chem.* **2001**, *8*, 121–133.
(31) Kelly, T. A.; McNeil, D. W. A simple method for the protection of aryl amines as their *t*-butylcarbamoyl (Boc) derivatives. *Tetrahedron Lett.* **1994**, *35*, 9003–9006.
(32) Venuti, M. C.; Stephenson, R. A.; Alvarez, R.; Bruno, J. J.; Strosberg, A. M. Inhibitors of cyclic AMP phosphodiesterase. 3. Synthesis and biological evaluation of pyrido and imidazolyl analogs of 1,2,3,5-tetrahydro-2-oxoimidazo[2,1-*b*]quinazoline. *J. Med. Chem.* **1988**, *31*, 2136–2145.
(33) Sreekanth, A.; Fun, H.-K.; Kurup, M. R. P. Structural and spectral studies of an iron(III) complex $[Fe(Pranthas)_2][FeCl_4]$ derived from 2-acetylpyridine-*N*(4),*N*(4)-(butane-1,4-diyl) thiosemicarbazone (HPranthas). *J. Mol. Struct.* **2005**, *737*, 61–67.
(34) Kowol, C. R.; Eichinger, R.; Jakupec, M. A.; Galanski, M.; Arion, V. B.; Keppler, B. K. Effect of metal ion complexation and chalcogen donor identity on the antiproliferative activity of 2-acetylpyridine *N*,*N*-dimethyl(chalcogen)semicarbazones. *J. Inorg. Biochem.* **2007**, *101*, 1946–1957.
(35) Pessoa, M. M. B.; Andrade, G. F. S.; Paoli Monteiro, V. R.; Temperini, M. L. A. 2-Formylpyridinethiosemicarbazone and methyl derivatives: spectroscopic studies. *Polyhedron* **2001**, *20*, 3133–3141.
(36) Bermejo, E.; Castifieiras, A.; Fostiak, L. M.; Garcia, I.; Llamas-Saiz, A. L.; Swearingen, J. K.; West, D. X. Synthesis; characterization and molecular structure of 2-pyridylformamide *N*(4)-dimethylthiosemicarbazone and some five-coordinated zinc(II) and cadmium(II) complexes. *Z. Naturforsch., B: Chem. Sci.* **2001**, *56*, 1297–1305.
(37) West, D. X.; Bain, G. A.; Butcher, R. J.; Jasinski, J. P.; Li, Y.; Pozdniakiv, R. Y. Structural studies of three isomeric forms of heterocyclic N(4)-substituted thiosemicarbazones and two nickel(II) complexes. *Polyhedron* **1996**, *15*, 665–674.
(38) Odenike, O. M.; Larson, R. A.; Gajria, D.; Dolan, M. E.; Delaney, S. M.; Karrison, T. G.; Ratain, M. J.; Stock, W. Phase I study of the ribonucleotide reductase inhibitor 3-aminopyridine-2-carboxaldehyde-thiosemicarbazone (3-AP) in combination with high dose cytarabine in patients with advanced myeloid leukemia. *Invest. New Drugs* **2008**, *26*, 233–239.
(39) *CRC Handbook of Chemistry and Physics*; Lide, D. R., Ed.; CRC Press: Boca Raton, FL, 2004.
(40) Kowol, C. R.; Reisner, E.; Chiorescu, I.; Arion, V. B.; Galanski, M.; Deubel, D. V.; Keppler, B. K. An electrochemical study of antineoplastic gallium, iron and ruthenium complexes with redox non-innocent α-N-heterocyclic chalcogensemicarbazones. *Inorg. Chem.* **2008**, *47*, 11032–11047.
(41) Richardson, D. R.; Kalinowski, D. S.; Richardson, V.; Sharpe, P. C.; Lovejoy, D. B.; Islam, M.; Bernhardt, P. V. 2-Acetylpyridine thiosemicarbazones are potent iron chelators and antiproliferative agents: redox activity, iron complexation and characterization of their antitumor activity. *J. Med. Chem.* **2009**, *52*, 1459–1470.
(42) Easmon, J.; Heinisch, G.; Hofmann, J.; Langer, T.; Grunicke, H. H.; Fink, J.; Purstinger, G. Thiazolyl and benzothiazolyl hydrazones derived from α-(*N*)-acetylpyridines and diazines: synthesis, antiproliferative activity and CoMFA studies. *Eur. J. Med. Chem.* **1997**, *32*, 397–408.
(43) West, D. X.; Swearingen, J. K.; Valdes-Martinez, J.; Hernandez-Ortega, S.; El-Sawaf, A. K.; Van Meurs, F.; Castineiras, A.; Garcia, I.; Bermejo, E. Spectral and structural studies of iron(III), cobalt(II,III) and nickel(II) complexes of 2-pyridineformamide *N*(4)-methylthiosemicarbazone. *Polyhedron* **1999**, *18*, 2919–2929.
(44) Mendes, I. C.; Soares, M. A.; dos Santos, R. G.; Pinheiro, C.; Beraldo, H. Gallium(III) complexes of 2-pyridineformamide thiosemicarbazones: cytotoxic activity against malignant glioblastoma. *Eur. J. Med. Chem.* **2009**, *44*, 1870–1877.
(45) Yuan, J.; Lovejoy, D. B.; Richardson, D. R. Novel di-2-pyridyl-derived iron chelators with marked and selective antitumor activity: in vitro and in vivo assessment. *Blood* **2004**, *104*, 1450–1458.
(46) Easmon, J.; Heinisch, G.; Holzer, W.; Rosenwirth, B. Novel thiosemicarbazones derived from formyl- and acyldiazines: synthesis, effects on cell proliferation, and synergism with antiviral agents. *J. Med. Chem.* **1992**, *35*, 3288–3296.
(47) Richardson, D. R.; Sharpe, P. C.; Lovejoy, D. B.; Senaratne, D.; Kalinowski, D. S.; Islam, M.; Bernhardt, P. V. Dipyridyl thiosemicarbazone chelators with potent and selective antitumor activity form iron complexes with redox activity. *J. Med. Chem.* **2006**, *49*, 6510–6521.
(48) Agrawal, K. C.; Lee, M. H.; Booth, B. A.; Moore, E. C.; Sartorelli, A. C. Potential antitumor agents. 11. Inhibitors of alkaline phosphatase, an enzyme involved in the resistance of neoplastic cells to 6-thiopurines. *J. Med. Chem.* **1974**, *17*, 934–938.
(49) McElhinney, R. S. Derivatives of thiocarbamic acid. I. Preparation of 4-substituted thiosemicarbazides. *J. Chem. Soc.* **1966**, *10*, 950–955.
(50) Castineiras, A.; Garcia, I.; Bermejo, E.; West, D. X. Structural and spectral studies of 2-pyridineformamide thiosemicarbazone and its complexes prepared with zinc halides. *Z. Naturforsch., B: Chem. Sci.* **2000**, *55*, 511–518.
(51) Barette, W. C., Jr.; Johnson, H. W., Jr.; Sawyer, D. T. Voltammetric evaluation of the effective acidities (pKa′) for Broensted acids in aprotic solvents. *Anal. Chem.* **1984**, *56*, 1890–1898.
(52) Sheldrick, G. M. *SHELXS-97, Program for Crystal Structure Solution*; University Gottingen: Gottingen, Germany, 1997.
(53) Sheldrick, G. M. *SHELXL-97, Program for Crystal Structure Refinement*; University Gottingen: Gottingen, Germany, 1997.
(54) Johnson, G. K. Report ORNL-5138; Oak Ridge National Laboratory; Oak Ridge, TN, 1976.
(55) *International Tables for X-ray Crystallography*; Kluwer Academic Press: Dodrecht, The Netherlands, 1992; Vol. C, Tables 4.2.6.8 and 6.1.1.4.
(56) Heffeter, P.; Jakupec, M. A.; Korner, W.; Wild, S.; von Keyserlingk, N. G.; Elbling, L.; Zorbas, H.; Korynevska, A.; Knasmuller, S.; Sutterluty, H.; Micksche, M.; Keppler, B. K.; Berger, W. Anticancer activity of the lanthanum compound [tris(1,10-phenanthroline)lanthanum(III)]trithiocyanate (KP772; FFC24). *Biochem. Pharmacol.* **2006**, *71*, 426–440.
(57) Szekeres, T.; Gharehbaghi, K.; Fritzer, M.; Woody, M.; Srivastava, A.; van't Riet, B.; Jayaram, H. N.; Elford, H. L. Biochemical and antitumor activity of trimidox, a new inhibitor of ribonucleotide reductase. *Cancer Chemother. Pharmacol.* **1994**, *34*, 63–66.